JETIR.ORG ISSN: 2349-5162 | ESTD Year : 2014 | Monthly Issue
JOURNAL OF EMERGING TECHNOLOGIES AND INNOVATIVE RESEARCH (JETIR)
An International Scholarly Open Access, Peer-reviewed, Refereed Journal

Green Fabrication of ZnO Nanoparticles from *Tridax procumbens* leaf extract: Antimicrobial and Cytotoxic Evaluation on MCF-7 and A549 Cells

A. Anantharaj[1], N. Rajkamal[1], G. Udhayakumar[1], B. Gokulakumar[1*]

[1] *PG & Research Department of Physics, Thiru. A. Govindasamy Government Arts College, Tindivanam-604307, Tamil Nadu, India.*

Abstract

In this present research, zinc oxide nanoparticles were prepared through an eco-friendly, sustainable green synthesis method utilizing *Tridax procumbens* leaf extract. Different analytical methods were used to carefully study the synthesis physicochemical properties of the biosynthesized TP-ZnO nanoparticles. The synthesized ZnO nanoparticles were validated by UV-visible spectroscopy, which exhibited a distinct absorption peak at 347 nm, despite FTIR analysis identifying functional groups that facilitate nanoparticle stability. Crystallization of hexagonal wurtzite in the synthesized nanoparticle structure was demonstrated by XRD studies. SEM analysis showed predominantly quasi-spherical morphology, and TEM analysis revealed spherical ZnO nanoparticles with particle sizes in the range of 7-15 nm, while elemental composition was verified through EDAX analysis. The biosynthesized ZnO nanoparticles exhibited significant antibacterial activity against Gram-positive and Gram-negative bacteria at different concentrations (500, 1000, and 200 µg) by using the disc diffusion method, with a maximum inhibition zone of 14 mm against P. aeruginosa. Anticancer activity evaluated by the MTT assay revealed IC_{50} values of 95.5 µg/mL for A459 cells and 29.72 µg/mL for MCF-7 cells. These findings indicate strong cytotoxic and antimicrobial potential of the nanoparticles. Overall, *Tridax procumbens*-mediated ZnO (TP-ZnO) nanoparticles demonstrate promising application in biomedical and pharmaceutical fields.

Keywords: Zinc oxide nanoparticle, Tridax procumbens, UV-vis spectroscopy, FTIR, SEM, TEM, EDAX, Antibacterial activity, Anticancer activity (A549, MCF-7 Cell lines)

1. Introduction

A variety of scientific disciplines, including chemistry, physics, biology, and engineering, are combined in the field of nanotechnology. It contributes to industrial growth, sustainable development, scientific innovation, etc. In this field, materials with sizes ranging from 1 to 100 nm are designed and

utilized for various applications. [1]. Nanomaterials possess peculiar properties like reactivity improvement, large surface area, and quantum effects. These properties differ from bulk materials [2]. Zinc oxide is a most interesting inorganic oxide, which is mostly used for the fabrication of devices. Zinc oxide is extensively applied in the fabrication of transistors, light-emitting diodes (LEDs), and quantum dot solar cells (QDSC). Due to its antibacterial, anticancer, antimicrobial, and anti-inflammatory properties, it is largely used in cosmetics, wound healing, drug delivery medical products, pharmaceuticals, and environmental safety [3]. Zinc oxide nanoparticles have a band gap energy of 3.37 eV and a high excitation binding energy of 60 meV, which serves as a high potential application [4]. Recently, zinc oxide nanoparticles are considered superior to other metal oxide nanoparticles due to their low toxicity, good bioavailability, low cost, high stability, and easy preparation methods. ZnO nanostructures have emerged as a major research focus because of their distinct properties and numerous applications [5]. Nanobiotechnology is an emerging interdisciplinary field that uses biological resources and nanofabrication techniques to produce environmentally friendly nanoscale materials and develop advanced devices for studying biological systems [6].

Green synthesis methods, unlike chemical and physical approaches, leverage herbs and microorganisms like bacteria, fungi, and algae, attracting considerable interest [7]. Plant extracts effectively produce both metal and metal oxide nanoparticles, supporting large-scale manufacturing without extra contaminants. This technique cuts down on hazardous solvents and reducing and stabilizing agents while advancing eco-friendly technologies for materials synthesis [8]. Previous studies have successfully created ZnO nanoparticles using extracts from medicinal plants like Andrographis paniculata [9], Senna auriculata [10], Leucas aspera [11], Azadirachta indica [12], Moringa oleifera [13], Solanum nigrum [14], and Eclipta prostrata [15]. The aim of this present work focuses on the green synthesis of *Tridax procumbens* aqueous leaf extract-mediated ZnO (TP-ZnO) nanoparticles. *Tridax procumbens* is located in fields, meadows, agricultural lands, lawns, and roadsides within tropical or semi-tropical climates, belongs to the family Asteraceae, and is commonly known as “coatbuttons” or “tridax daisy” and “Vettukaaya-poondu” (Tamil/Siddha) [16,17,18]. In India, *Tridax procumbens* has been traditionally used in ayurvedic medicine as an herbal treatment for wound healing [19]. It has also been applied by local healers for managing boils, blisters, and minor cuts. *Tridax procumbens* is a very important plant that may be found all over the world [20]. It has hygienic properties. This plant is utilized by individuals in India as a source of food or medicine [21]. And used to treat liver diseases [22], prevent hair loss, and promote hair growth [23]. also treat several illnesses since ancient times. A wide range of bioactive substances, such as flavonoids, alkaloids, tannins, saponins, steroids, terpenoids, and carotenoids, are present in this plant [24]. The constituents are responsible for providing it with numerous biological activities, such as antifungal, antibacterial, anticancer, antioxidant, anti-inflammatory, antileishmanial, immunomodulatory, vasorelaxant, larvicidal, anthelmintic, and antiseptic [18]. Cancer is a major threat to human health worldwide, causing a high mortality rate. Conventional chemotherapy is limited by low specificity and dose-related side effects, which may lead to long-term health problems such as organ damage and fertility issues [25]. Therefore, eco-friendly, green-synthesized nanoparticles are being explored as a promising alternative for targeted and controlled cancer

treatment [26]. This study explored the environmentally friendly creation of ZnO nanoparticles using extracts from *Tridax procumbens* leaves, and it examined their effectiveness against both gram-positive and gram-negative bacteria, as well as their cytotoxicity on the A549 and MCF-7 cell lines.

2. Materials and methods

2.1 Plant and chemical collection

Fresh and healthy leaves of *Tridax procumbens* were collected from agricultural land in Thaiyur village, Villupuram District, Tamil Nadu, India. The collected leaves were thoroughly washed with tap water followed by deionized water to remove dust and surface impurities and then shade-dried at room temperature. Analytical grade zinc acetate dihydrate ($Zn(CH_3COO)_2 \cdot 2H_2O$) and sodium hydroxide (NaOH) were procured from Merck India and used without further purification. Deionized water was employed as the solvent throughout the synthesis process

2.2 Preparation of leaf extract

Fresh leaves of *Tridax procumbens* were collected and thoroughly washed with deionized water to remove adhering impurities, then shade-dried at room temperature for 10-15 days to preserve the bioactive compounds and ensure the formation of stable phytochemicals for nanoparticle synthesis. After drying, the leaves were finely crushed and powdered using a mechanical grinder. For the preparation of the aqueous extract, 10 g of the powdered leaf material was mixed with 100 ml of deionized water and heated at 60-70 °C for 60 min under continuous stirring. The resulting extract was allowed to cool to room temperature and subsequently filtered using Whatman No. 1 filter paper to remove solid residues. The obtained filtrate was collected and stored at 4°C for further experimental use.

2.3 Biosynthesis of ZnO nanoparticles from Tridax procumbens leaf (TP-ZnO)

The biosynthesis of ZnO nanoparticles was performed by mixing 50 ml of an aqueous solution of 0.4 M zinc acetate dihydrate with 10 ml of *Tridax procumbens* leaf extract under continuous magnetic stirring for 1 h. Subsequently, 50 ml of an aqueous solution of 0.2 M NaOH was added dropwise to the reaction mixture while maintaining constant stirring. The reaction mixture was further stirred for 2 h, during which the formation of a greenish-white suspension was observed, indicating the synthesis of ZnO nanoparticles. The obtained suspension was allowed to stand undisturbed at room temperature for 12 h to facilitate complete settling of the precipitate. The settled precipitate was separated by decantation and repeatedly washed with deionized water followed by ethanol to remove unreacted precursors and residual phytochemicals. The purified product was then dried in a hot air oven at 80°C for 12 h to obtain ZnO nanoparticles, as shown in Fig. 1.

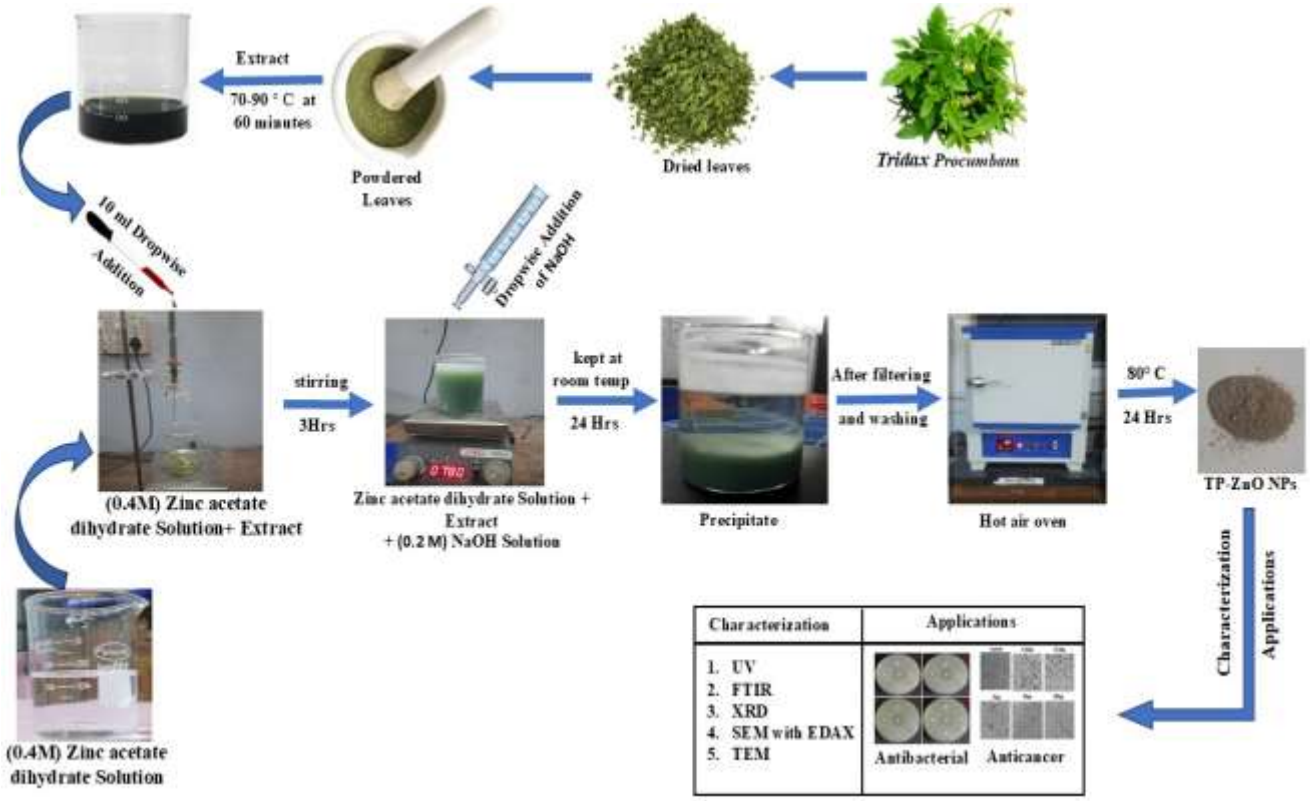

Fig. 1. Biosynthesis of ZnO nanoparticles from Tridax procumbens leaf (TP-ZnO)

2.4 Antibacterial activities by the Disc-Diffusion method

The antibacterial activity of synthesized TP-ZnO nanoparticles was evaluated against selected Gram-negative bacteria (*Pseudomonas aeruginosa and Escherichia coli*) and Gram-positive bacteria (*Bacillus subtilis and Staphylococcus aureus*) using the disc diffusion technique. The test microorganisms were initially grown in nutrient broth and incubated at 37°C for 24 h to obtain actively growing cultures. The bacterial suspensions were then diluted and uniformly spread on Petri plates containing nutrient agar medium. Sterile discs were placed on the surface of the inoculated agar plates and impregnated with ZnO nanoparticle samples at concentrations of 500, 1000, and 2000 µg. A disc loaded with streptomycin (20 µg) was used as the positive control to evaluate the sensitivity of the tested bacterial strains. The prepared plates were incubated at 37°C for 24 h. After incubation, the antibacterial effectiveness was assessed by measuring the diameter of the clear inhibition zones formed around each disc, and the values were recorded in millimeters.

2.5 MTT assay

The in vitro cytotoxic activity of Tridax procumbens-mediated ZnO nanoparticles was evaluated using the MTT assay. MTT reagent and dimethyl sulfoxide (DMSO) were used for the detection and solubilization of formazan crystals. The experiment was carried out using a CO_2 incubator, a microplate reader, and an inverted microscope. Test samples of ZnO nanoparticles were dispersed in culture medium and prepared in serial two-fold dilutions with concentrations ranging from 6.25 to 100 µg/mL. Human breast cancer (MCF-7) and lung cancer (A549) cell lines were obtained from NCCS, India, and maintained in DMEM supplemented with 10% fetal bovine serum and penicillin (100 IU/mL) at 37°C in a humidified

atmosphere containing 5% CO_2. Exponentially growing cells were harvested by trypsinization and adjusted to a concentration of 1.0 x 10^5 cells/mL. Then, 100 µL of the cell suspension (1 x 10^4 cells/well) was seeded into 96-well plates and incubated for 24 h for cell attachment. After incubation, the cells were treated with different concentrations of ZnO nanoparticles and further incubated for 24 h. Following treatment, the culture medium was removed, and 20 µL of MTT solution (2 mg/mL in PBS) was added to each well. The plates were incubated for 4 h to allow formazan crystal formation. The supernatant was then discarded, and 100 µL of DMSO was added to dissolve the crystals completely. Absorbance was measured at 570 nm using a microplate reader, and the cell viability was calculated by comparing the absorbance of treated cells with that of untreated control cells using the following equation.

$$\% \, viability = \frac{Sample \; absorption}{Control \; absorption} \times 100$$

2.6 Characterization

The optical properties of Tridax procumbens-mediated zinc oxide nanoparticles were analyzed using a UV-visible spectrometer (Lambda 35, PerkinElmer) in the range of 200 nm to 800 nm. Functional groups associated with plant-derived biomolecules were identified by FT-IR spectroscopy (Spectrum RX I, PerkinElmer) in the range of 4000 cm^{-1} to 400 cm^{-1}. The crystalline nature of the nanoparticles was examined by X-ray diffraction (Bruker D8 diffractometer) in the range of 2θ = 20°–80°. The surface morphology was observed using Scanning Electron Microscopy (SEM) (ZEISS: EVO18), and elemental composition was determined by Energy Dispersive X-ray Analysis (EDAX). The size and shape of the nanoparticles were further investigated using Transmission Electron Microscopy (TEM) (Talos F200S).

3. Result and discussion

3.1 UV-Visible analysis

Fig. 2. The UV-visible spectrum of *Tridax procumbens* leaf extract-mediated ZnO nanoparticles (TP-ZnO) shows a characteristic absorption peak at 347 nm, which is attributed to the characteristic band gap absorption of ZnO nanoparticles. The optical band gap energy, estimated using the Tauc relation for direct band gap semiconductors, was found to be 3.57 eV. The increase in the band gap energy compared to bulk ZnO (~3.37 eV) indicates a pronounced blue shift [27], which can be attributed to quantum confinement effects and the nanoscale particle formation. The presence of phytochemicals in the Tridax procumbens leaf extract is thought to be very important for lowering and stabilizing ZnO nanoparticles. These results confirm the successful biosynthesis of TP-ZnO nanoparticles.

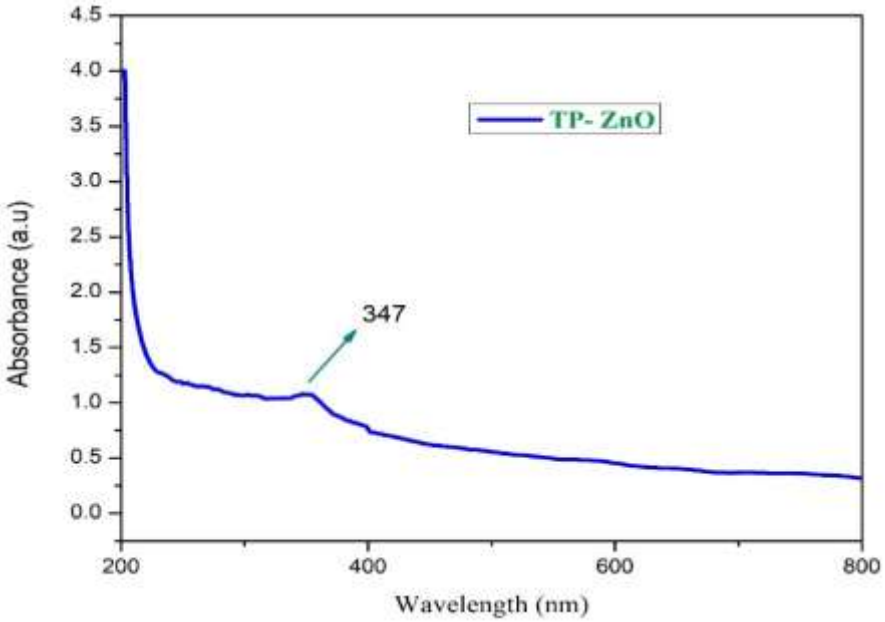

Fig. 2. UV-visible absorption spectrum of TP-ZnO nanoparticles.

3.2 FTIR analysis

Fourier Transform Infrared (FTIR) spectroscopy was employed to investigate the functional groups present in the synthesized *Tridax procumbens* leaf extract with ZnO nanoparticles. The FTIR spectrum recorded in the range of 4000–500 cm^{-1} is shown in Fig. 3.

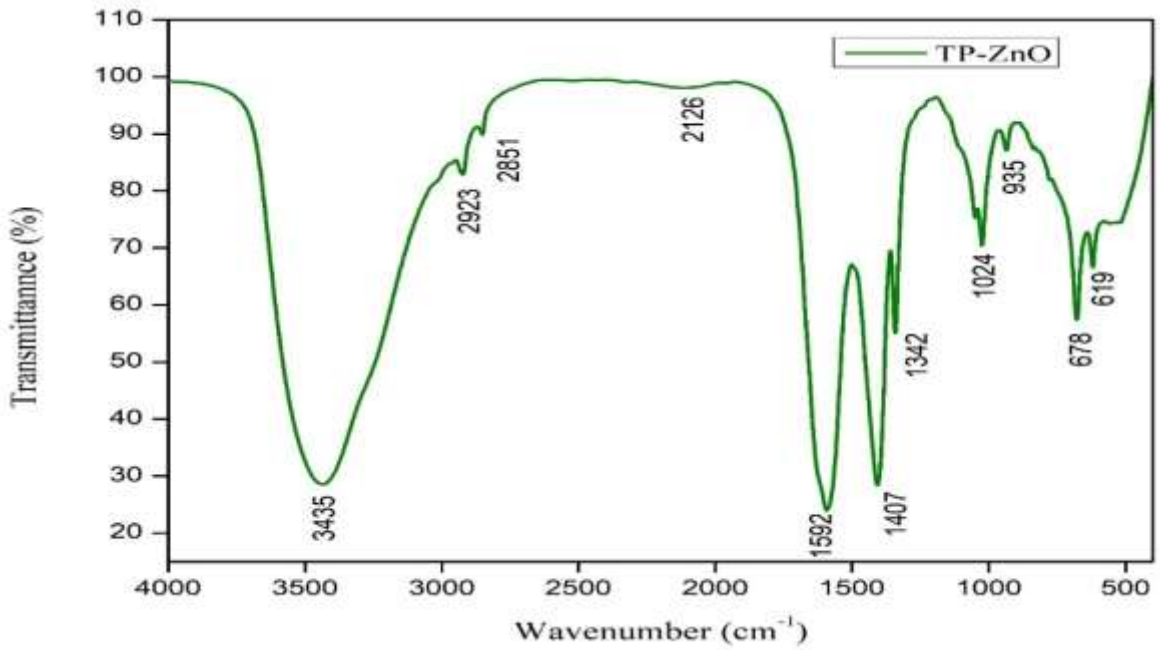

Fig. 3. FTIR Spectral analysis of TP-ZnO Nanoparticles

A broad and intense absorption band observed at 3435 cm^{-1} is attributed to O–H stretching vibrations, indicating the presence of surface-adsorbed water molecules and hydroxyl groups. This band confirms the hydrophilic nature of the ZnO surface and possible hydrogen bonding interactions. The peaks appearing at 2923 cm^{-1} and 2851 cm^{-1} correspond to asymmetric and symmetric C–H stretching vibrations. These organic residues likely act as reducing and stabilizing agents. A weak band observed at 2126 cm^{-1} may be attributed to C≡C stretching vibrations or possible residual organic functional groups. The strong

absorption band at 1592 cm^{-1} is assigned to C=O stretching or O–H bending vibrations, indicating the presence of carbonyl-containing compounds.

Table 1. FTIR assignment of *Tridax procumbens* leaf extract with ZnO nanoparticles.

FTIR Assignment	Frequency range (cm^{-1}) of TP-ZnO	Reference frequency range (cm^{-1})	Chemical bond	Groups and structures
1	3435	3500 - 3200	O-H stretching vibrations	Phenols and alcohols
2	2923 and 2851	3000-2850	C-H stretching	Alkanes groups
3	2126	2260-2100	C≡ C (carbon-carbon triple bond)	Alkyne groups
4	1592	1595-1590	C = C (carbon-carbon double bond)	Alkene groups
5	1407	1411-1407	C-N Stretching	Carboxylate groups
6	1342	1350-1340	C–H bending vibrations	Alkanes groups
7	1024	1250-1020	C–O Stretching vibrations	Alcohol, Ether
8	935	950-910	Zn–OH and other metal–oxygen vibration modes.	Metal–hydroxide group
	678	690-515		
9	619	700-600	Zn–O stretching vibrations	Inorganic metal–oxygen

The band at 1407 cm^{-1} corresponds to C–N stretching or symmetric stretching of carboxylate groups, further supporting the involvement of biomolecules in nanoparticle stabilization. The peak at 1342 cm^{-1} may be attributed to C–H bending vibrations. The absorption band at 1024 cm^{-1} is assigned to C–O stretching vibrations of alcohols, phenols, or ethers present in the plant extract. The bands observed at 935 cm^{-1} and 678 cm^{-1} are associated with Zn–OH and other metal–oxygen vibrational modes. Importantly, the characteristic strong absorption band at 619 cm^{-1} confirms the presence of Zn–O stretching vibrations, which validates the successful formation of ZnO nanoparticles as shown in Table 1. Overall, the FTIR results confirm the synthesis of ZnO nanoparticles and indicate that phytochemical constituents present in the *Tridax procumbens* leaf extract play a significant role in the reduction, capping, and stabilization of the nanoparticles [28].

3.3 XRD analysis

X-ray diffraction analysis of *Tridax procumbens* leaf extract with zinc oxide nanoparticles gives information about crystallinity, structure, and average particle size. The XRD patterns of *Tridax procumbens* leaf with ZnO are shown in Fig. 4. The peaks exhibited sharp diffraction angles at 2Θ values of 31.42, 34.51, 36.23, 47.65, 57.61, 62.78, and 68.03, which could be recorded in the lattice planes (100), (002), (101), (102), (110), (103), and (112), respectively, for low and high intensity. As a result, the presence of these prominent peaks in ZnO nanoparticles suggests that their structures are robust and their diffraction is pronounced. The findings confirm that the ZnO nanoparticles (NPs) exhibit a hexagonal wurtzite crystal structure arrangement. Furthermore, the distinct sharp Bragg peaks detected are attributed to the stabilizing effect of the capping agent used during synthesis. Thus, XRD analysis indicates the crystallinity of ZnO nanoparticles, showing patterns comparable to JCPDS (No. 36-1451) and in agreement with earlier reports [29, 30].

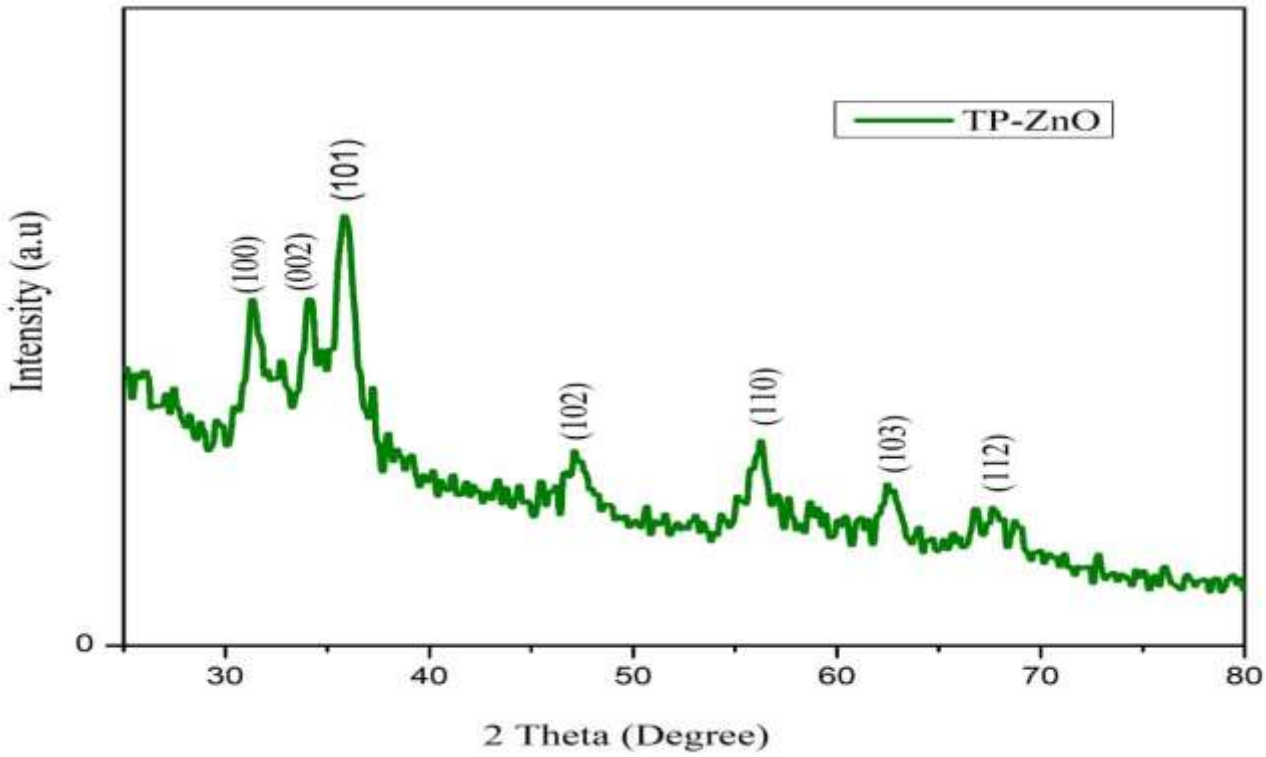

Fig. 4. XRD patterns of TP-ZnO nanoparticles.

The average crystallite size of the ZnO nanoparticles was calculated using the Debye-Scherrer equation, based on their peak positions, full width at half maximum, and wavelength of the incident radiation. The relationship for the average crystallite size D is expressed as follows:

$$D=k\lambda / \beta \cos \Theta$$

Where k, λ, β, and Θ represent the Scherrer constants (0.89), the X-ray wavelength of Cu-Kα, the full width at half maximum (FWHM) of the diffraction angles (in radians), and the Bragg angle (in degrees), respectively [31]. Evaluation of the average crystallite size of the TP-ZnO nanoparticles values 11.03 nm, as shown in Table 2. The ZnO nanoparticles synthesized with *Tridax procumbens* are phase-pure with no detectable impurities. The crystallite size can be estimated, confirming nanoscale formation, and peaks

indicate good quality of crystallinity, suggesting effective biomolecule-mediated stabilization. Finally, Tridax procumbens leaf extract contributes to controlled particle growth and prevents amorphous or aggregated formation.

Table 2. Evaluation of Crystallite sizes of TP-ZnO nanoparticles from XRD data

SL.No.	2Θ	Θ	COS Θ	FWHM	$\beta = \pi/180^{\circ}$ (FWHM)	$D = K\lambda / \beta \cos\Theta$
1	31.42	15.71	0.9626	0.5904	10.272	13.9779
2	34.51	17.25	0.9550	0.5904	10.272	14.0899
3	36.23	18.11	0.9504	0.6888	11.985	12.1349
4	47.65	23.82	0.9148	0.9840	17.121	8.8255
5	57.61	28.80	0.8763	0.7872	13.697	11.5168
6	62.78	31.39	0.8536	0.7872	13.697	11.8220
7	68.03	34.01	0.8289	1.9680	34.243	4.8700
					Average Crystallites Size (D)	11.03 nm

3.4 SEM with EDAX analysis

The surface morphology and aggregation behavior of *Tridax procumbens*-mediated ZnO nanoparticles (TP-ZnO) were examined using scanning electron microscopy (SEM). Fig. 5 (a-b) shows the SEM images of TP-ZnO nanoparticles recorded at various magnifications, which display quasi-spherical ZnO nanoparticles with an agglomerated cluster-like morphology and particle sizes that are in good accordance with earlier reports on plant-mediated ZnO nanoparticles [32]. At which lower magnification (Fig. 5a) revealed irregularly shaped, loosely packed agglomerates, indicating a natural tendency for nanoparticle clustering. This agglomeration is commonly observed in green-synthesized metal oxide nanoparticles and can be attributed to interparticle interaction as well as the capping effect of plant-derived phytochemicals present on the nanoparticles' surface. A high-magnification SEM image (Fig. 5b) provided detailed insight into the nanoscale features within the agglomerates. These images demonstrated that the clusters were composed of fine, predominantly spherical nanoparticles.

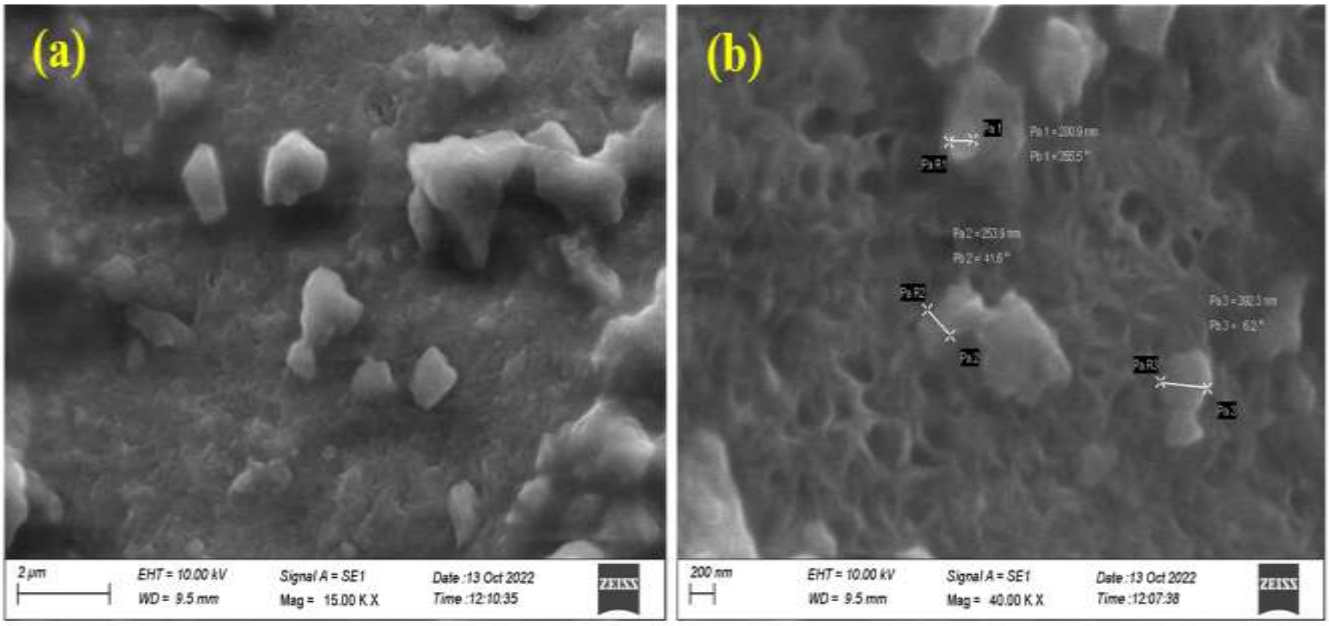

Fig. 5. SEM Micrograph of TP-ZnO Nanoparticles

Energy dispersive X-ray analysis (EDAX) was carried out to determine the elemental composition and purity of the synthesized ZnO nanoparticles, as shown in Fig. 6. The EDAX spectrum exhibits prominent characteristic peaks corresponding to zinc (Zn) and oxygen (O), confirming the formation of ZnO. The intense peak appearing at ~1.0 keV and near ~8.6 to 9.0 keV clearly indicates the presence of zinc, while the oxygen peak appearing at ~0.52 keV confirms the oxide phase [33].

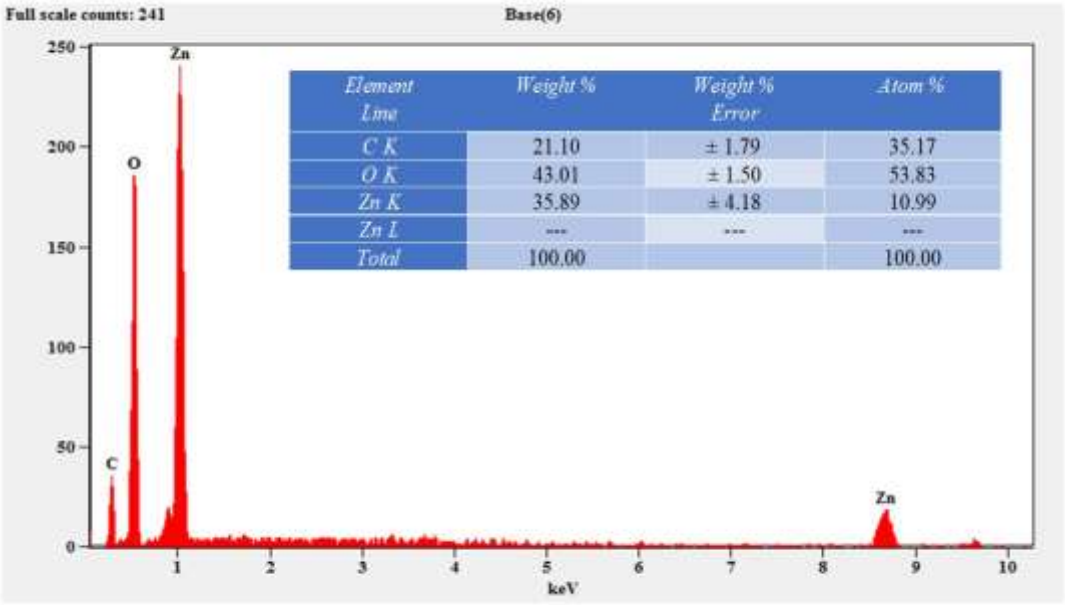

Fig. 6. Elemental Composition Analysis of TP-ZnO Nanostructures using EDAX

Additionally, the quantitative analysis indicated the weight percentages of Zn (35.89%) and O (43.01%) are in good agreement with the previously reported green synthesis of ZnO nanoparticles [34]. A minor carbon peak (21.10%) was also detected, attributed to Tridax procumbens plant-derived organic compounds used during analysis [35]. No impurity elements were observed, confirming the purity of the ZnO nanoparticles.

3.5 TEM analysis

TEM micrographs of *Tridax procumbens* leaf extract-mediated TP-ZnO nanoparticles are shown in Fig. 7 (a-c), which display nearly spherical shapes with an average particle size found to be in the range of 7–15 nm, confirming the successful formation of nanosized ZnO particles. The corresponding SAED pattern shows (Fig. 7-d) well-defined concentric diffraction fringes indexed to the (100), (002), and (101) planes of the hexagonal wurtzite structure ZnO, confirming the crystalline and polycrystalline nature of the nanoparticles and good agreement with XRD results.

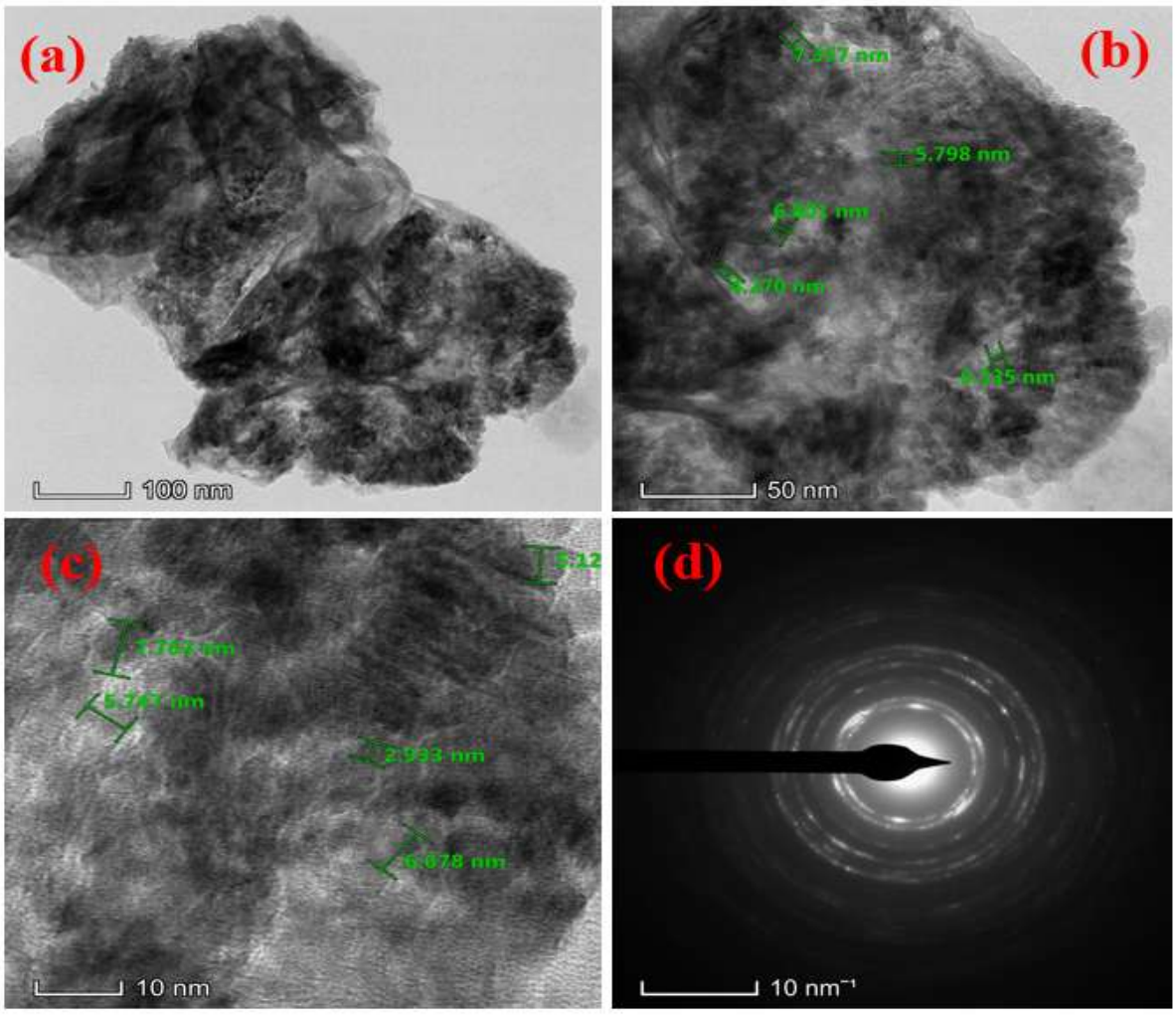

Fig. 7. (a-c) TEM images of TP-ZnO nanoparticles at various magnifications showing particle morphology and size distribution; (d) SAED patterns confirming the crystalline nature of the synthesized nanoparticles.

3.6 Antibacterial activity

The antibacterial efficacy of *Tridax procumbens* leaf extract-mediated ZnO nanoparticles (TP-ZnO) was investigated by the disc diffusion method against *E. coli*, *P. aeruginosa*, *B. subtilis*, and *S. aureus* with streptomycin as the positive control; it is shown in Fig. 8. At 500 µg/disc, negligible activity was noted, except for S. aureus. Moderate inhibition zones (9-10 mm) were observed at 1000 µg/disc. Maximum antibacterial activity was achieved at 2000 µg/disc, with inhibition zones ranging from 12 to 14 mm, and these calculated values are tabulated in Table 3, which indicates a clear concentration-dependent antibacterial effect of TP-ZnO NPs. From the above results, the antibacterial response of TP-ZnO

nanoparticles varied between Gram-negative bacteria (*E. coli* and *P. aeruginosa)* and Gram-positive (B. *subtilis and S. aureus*). Gram-negative strains exhibited slightly higher sensitivity, particularly P. aeruginosa, which showed the largest inhibition zone (14 mm), which is shown in Fig. 9. The antibacterial activity is attributed to the synergistic interaction of ZnO nanoparticles and bioactive phytochemicals present in *Tridax procumbens*, leading to membrane damage, oxidative stress, and bacterial growth suppression [36-38].

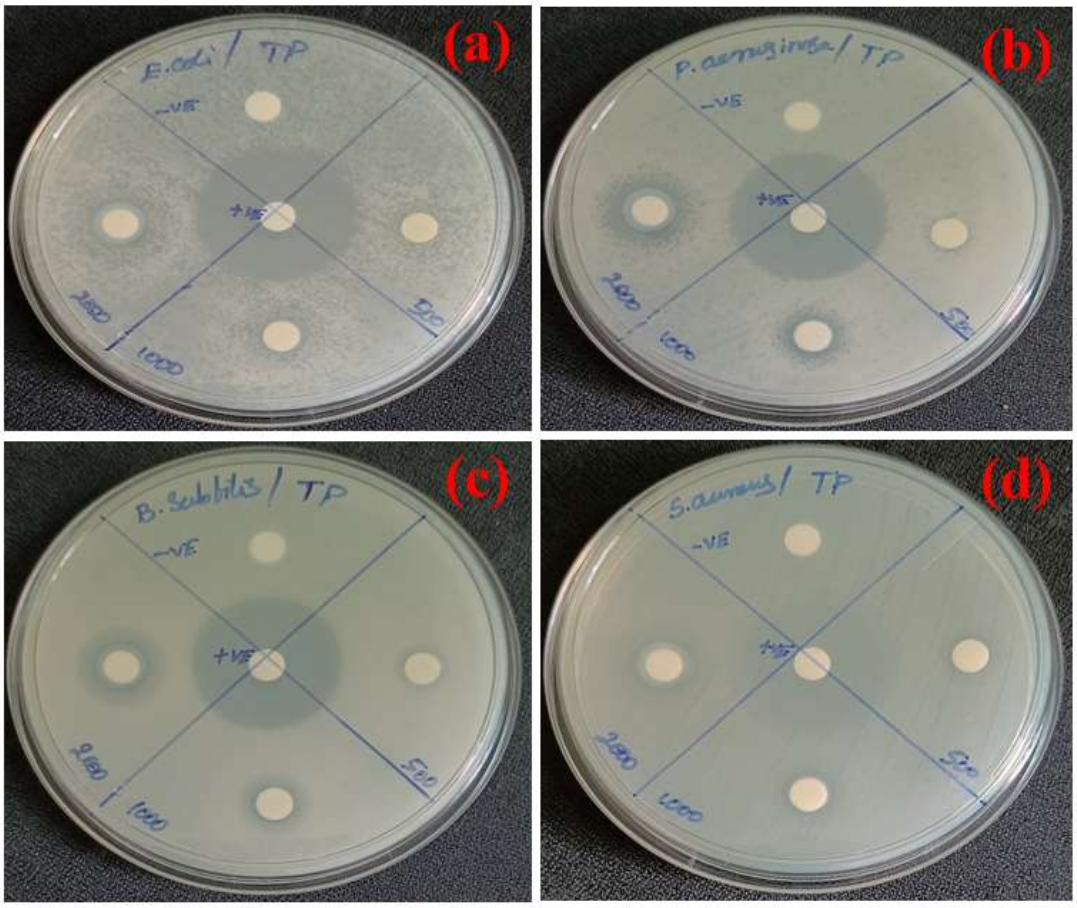

Fig. 8. Photographic images of the antibacterial activity of TP-ZnO nanoparticles against a) *E. coli,* b) *P. aeruginosa,* c) *B. subtilis*, and d) *S. aureus* at different concentrations (500, 1000, and 2000 µg).

Table 3. Zone of inhibition for antibacterial assay

Pathogenic microorganism	Zone of inhibition (mm)				
	Control	500µg	1000 µg	2000 µg	Positive control
E. Coli	-	-	9	12	26
P. aeruginosa	-	-	10	14	26
B. Subtilis	-	-	10	12	24
S. aureus	-	8	10	12	26

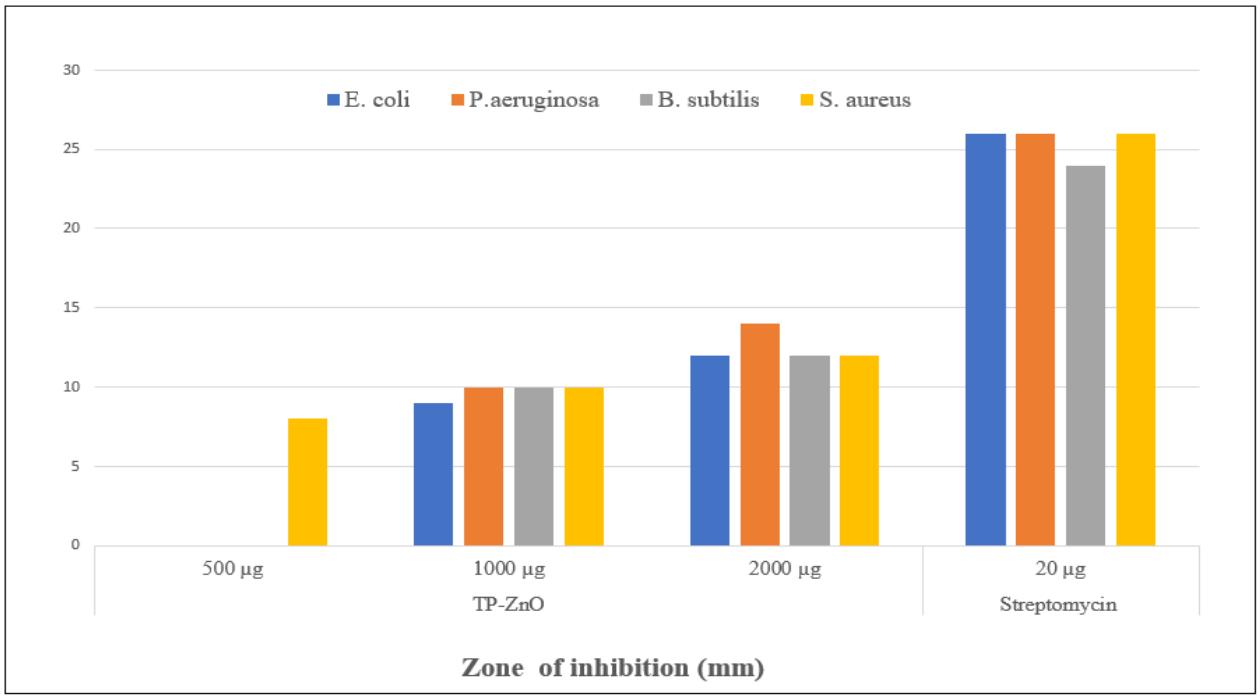

Fig. 9. Concentration-dependent antibacterial response of TP-ZnO nanoparticles (bar diagram), with positive control (Streptomycin).

3.7 Anticancer activity

The in vitro anticancer efficacy of *Tridax procumbens* leaf extract-mediated ZnO nanoparticles (TP-ZnO) at various concentrations (6.25, 12.5, 25, 50, 100 µg/mL) was evaluated against lung adenocarcinoma (A549) and human breast cancer (MCF-7) cell lines using the MTT assay. Cisplatin and 5-Fluorouracil (5-FU) were employed as standard anticancer drugs for A549 and MCF-7 cells, respectively, for comparison.

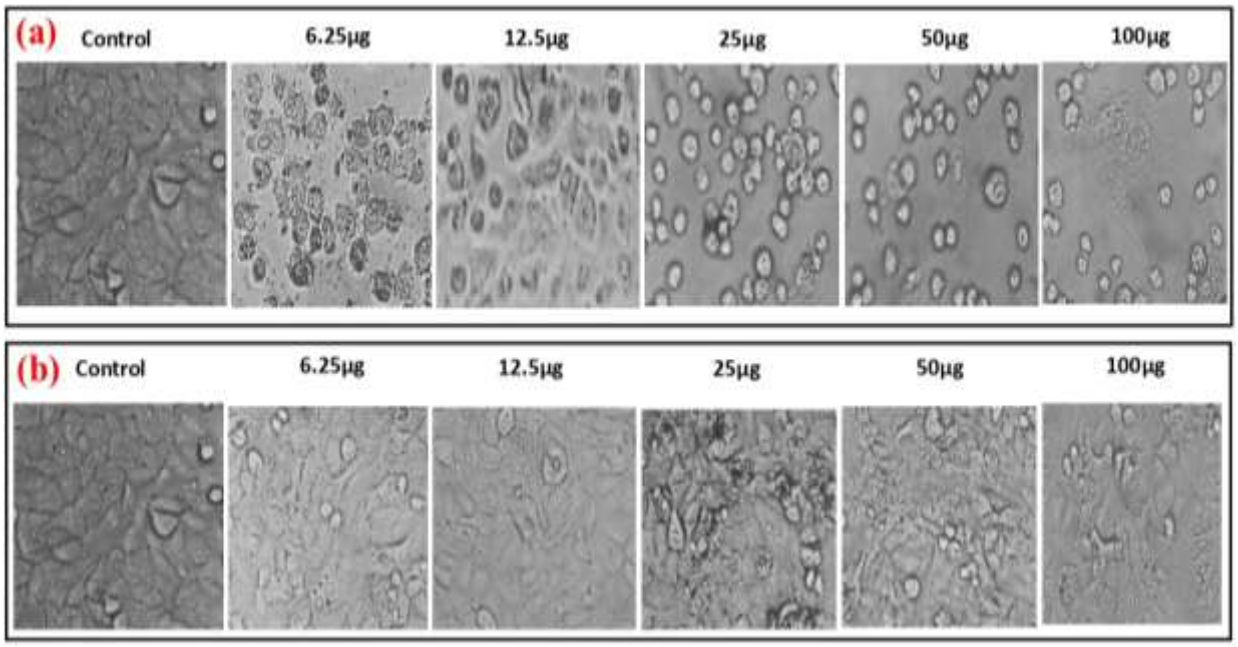

Fig. 10. Microscopic observation of lung cancer cells (A549) Following treatment with a) Standard drug (cisplatin) and b) TP-ZnO NPs at increasing concentrations.

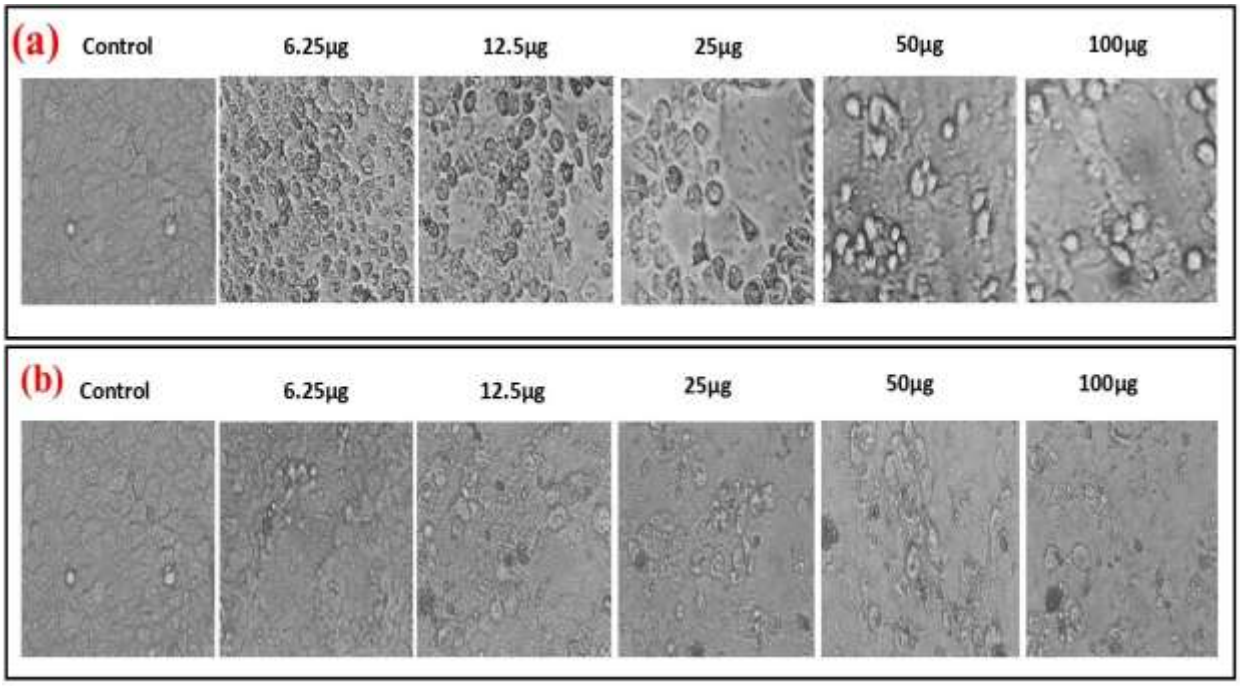

Fig. 11. Microscopic observation of breast cancer cells (MCF-7). Following treatment with a) reference standard (5FU) and b) TP-ZnO NPs at increasing concentrations.

With the optical micrographs, a clear dose-dependent reduction in cell viability was observed for both cell lines upon TP-ZnO treatment, as illustrated in Figs. 10 & 11**.** As the nanoparticle concentration increased, pronounced morphological alteration became evident, including cell shrinkage, loss of filopodial extensions, cellular rounding, and reduced structural integrity [39, 40]. At higher concentrations, a substantial decline in viable cells was observed, indicating strong cytotoxic activity of TP-ZnO nanoparticles.

Cell viability was quantitatively assessed using the MTT assay, and a dose-response curve was constructed to evaluate the cytotoxic effect of TP-ZnO nanoparticles, as shown in Fig. 12. For A549 cells, TP-ZnO nanoparticles demonstrated an IC_{50} value of 95.5 µg/mL, while cisplatin, used as the standard drug, exhibited an IC_{50} value of 7.07 µg/mL. In the case of MCF-7 cells, TP-ZnO nanoparticles exhibited an IC_{50} value of 29.72 µg/mL, whereas the standard chemotherapeutic drug 5-Fluorouracil (5-FU) showed a significantly lower IC_{50} value of 8.18 µg/mL, indicating higher cytotoxic potency of the standard drug.

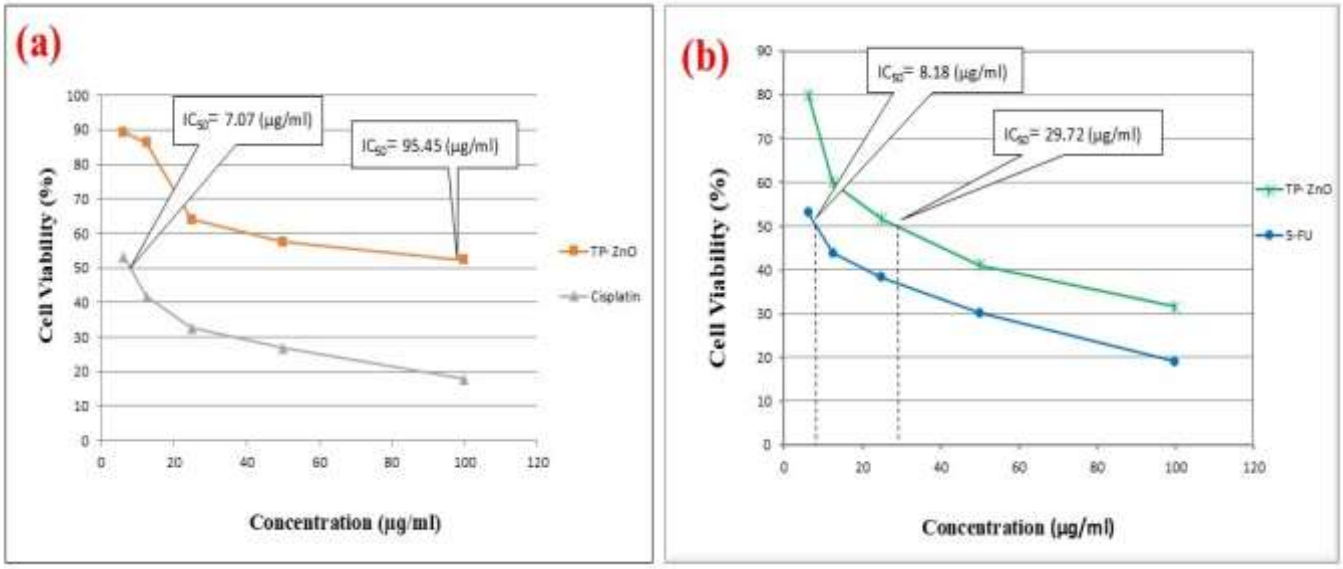

Fig. 12. IC_{50} determination and dose-response curves illustrating the viability of A549 (a) and MCF-7 (b) cells, compared with the standard reference drug at varying concentrations.

TP-ZnO nanoparticles exhibited a clear concentration-dependent reduction in cell viability in both A549 and MCF-7 cancer cell lines, as represented in the bar diagram in Fig. 13. With increasing TP-ZnO concentration, a gradual decline in viable cells was observed, confirming dose-response behavior.

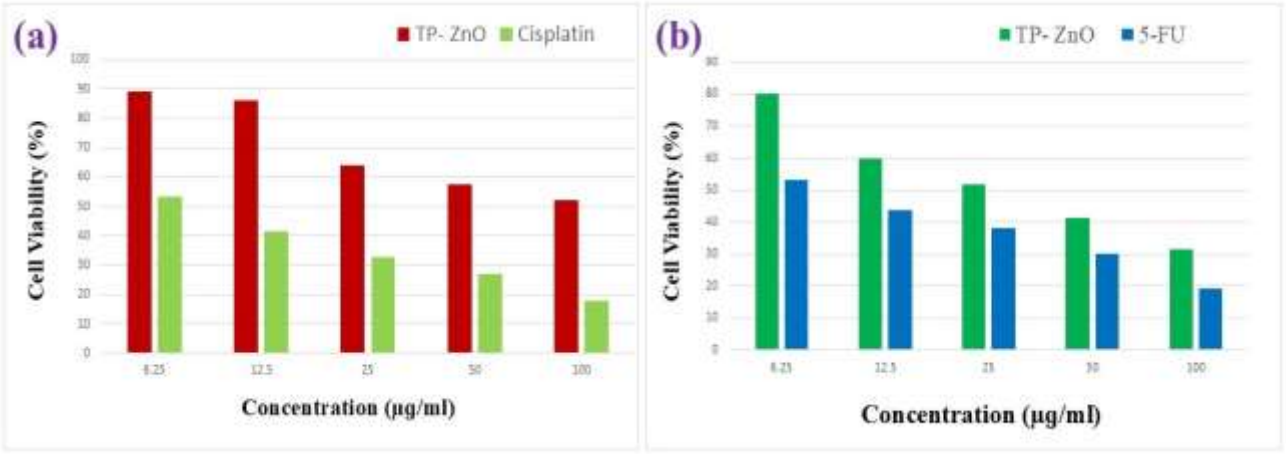

Fig. 13. Bar diagram showing the concentration-dependent reduction in cell viability of TP-ZnO nanoparticles in a) A549 and standard drug (Cisplatin) b) MCF-7 and standard drug (5-FU)

MCF-7 cells showed a steeper decline in viability compared to A549 cells, indicating higher sensitivity. The IC_{50} value for TP-ZnO was 29.72 µg/mL in MCF-7, whereas a significantly higher concentration (95.5 µg/mL) was required to achieve similar inhibition in A549 cells. This differential response highlights the selective anticancer potential of TP-ZnO nanoparticles. The lower IC_{50} value obtained for MCF-7 cells (29.72 µg/mL) compared to A549 cells (95.5 µg/mL) suggests a higher susceptibility of breast cancer cells to TP-ZnO-induced cytotoxicity. This difference may be related to variations in cellular metabolism, antioxidant defense mechanisms, and nanoparticle internalization efficiency.

ZnO nanoparticles are known to induce cancer cell death primarily through reactive oxygen species (ROS) generation, leading to oxidative stress, mitochondrial dysfunction, and activation of apoptosis

pathways [41]. The presence of *Tridax procumbens* phytochemicals is believed to further enhance ROS production and apoptotic signaling, thereby improving anticancer efficacy.

4. Conclusion

This study demonstrates the successful green synthesis of zinc oxide nanoparticles using *Tridax procumbens* extract, as indicated by a UV-vis absorption peak at 347 nm and a band gap value of 3.57 eV. The involvement of plant-derived functional groups in nanoparticle stabilization was confirmed by FTIR analysis. Particle sizes ranging from 7 to 15 nm were determined through XRD and TEM analysis. SEM images exhibited a quasi-spherical morphology with a strong tendency to form irregular agglomerated clusters, and elemental composition was verified by EDAX. Antibacterial activity was evaluated against both Gram-negative (*E. coli*, *P. aeruginosa)* and Gram-positive (*B. subtilis and S. aureus)* bacteria using streptomycin as a positive control at different concentrations (500, 1000, and 2000 µg). Notably, the nanoparticles exhibited significant antibacterial efficacy, with the highest zone of inhibition (14 mm) observed against *P. aeruginosa.* Anticancer potential was evaluated against human lung cancer (A549) and human breast cancer (MCF-7) cell lines using the MTT assay across concentrations from 6.25 to 100 µg/mL.

IC_{50} values were determined as 29.72 µg/mL for 95.5 µg/mL for A549 cells (with cisplatin standard: 7.07 µg/mL) and MCF-7 cells (5-FU: 8.18 µg/mL), indicating that MCF-7 cells exhibited higher sensitivity. In summary, the investigation demonstrates that *Tridax procumbens*-mediated ZnO nanoparticles (TP-ZnO NPs) have desirable physicochemical traits and significant biological functions. The nanoparticles showed the best antibacterial effects against *P. aeruginosa* and exhibited superior anticancer activity against the MCF-7 cell line, supporting their potential application in antimicrobial and anticancer therapies.

Author's Declaration

The authors declare that they have no known competing financial interest or personal relationship that could have appeared to influence the work reported in this paper.

Data Availability Statement

All data are contained within the manuscript and supporting document

Author's Contribution Statement

A. Anantharaj: Conceptualization, Methodology, Writing-Review & Editing, Data Curation, Formal Analysis, Software, Writing-Original Draft, Investigation.

N. Rajkamal: Methodology, Data Curation, Formal Analysis, Investigation.

G. Udhayakumar: Methodology, Data curation, Formal analysis, Investigation.

B. Gokulakumar: Conceptualization, Methodology, Visualization, Validation, Supervision, Writing-review & Editing.

References

[1] Navneet Phogat, Matthias Kohl, Imran Uddin, Afroz Jahan. Chapter 11—Interaction of Nanoparticles with Biomolecules, Protein, Enzymes, and Tts Applications. Precision medicine. 2018, Pages 253-276. DOI: https://doi.org/10.1016/B978-0-12-805364-5.00011-1

[2] Sahoo, S. K., et al. (2020). Nanotechnology in drug delivery. *Journal of Controlled Release*, 327, 285–307.

[3] Biomedical Materials & Devices https://doi.org/10.1007/s44174-025-00629-2

[4] M Junaid, S Ghulam Hussain, N Abbas, W Qamar khan, Band gap analysis of zinc oxide for potential bio glucose sensor. Results in Chemistry, Volume 5, 2023, 100961, ISSN 2211-7156, https://doi.org/10.1016/j.rechem.2023.100961

[5] Jha S, Rani R, Singh S. Biogenic Zinc Oxide Nanoparticles and Their Biomedical Applications: A Review. J Inorg Organomet Polym Mater. 2023 Apr 20:1-16. https://doi.org/10.1007/s10904-023-02550-x

[6] Raveendran P, Fu J, Wallen SL. Completely "green" synthesis and stabilization of metal nanoparticles. J Am Chem Soc. 2003 Nov 19;125(46):13940-1. https://doi.org/10.1021/ja029267j. PMID: 14611213

[7] El-Seedi HR, Omara MS, Omar AH, Elakshar MM, Shoukhba YM, Duman H, Karav S, Rashwan AK, El-Seedi AH, Altaleb HA, Gao H, Saeed A, Jefri OA, Guo Z, Khalifa SAM. Updated Review of Metal Nanoparticles Fabricated by Green Chemistry Using Natural Extracts: Biosynthesis, Mechanisms, and Applications. Bioengineering (Basel). 2024 Oct 30; 11(11): 1095. https://doi.org/10.3390/bioengineering11111095 (7) this above 18

[8] Singh H, Desimone MF, Pandya S, Jasani S, George N, Adnan M, Aldarhami A, Bazaid AS, Alderhami SA. Revisiting the Green Synthesis of Nanoparticles: Uncovering Influences of Plant Extracts as Reducing Agents for Enhanced Synthesis Efficiency and Its Biomedical Applications. Int J Nanomedicine. 2023 Aug 18; 18:4727-4750. https://doi.org/10.2147/IJN.S419369

[9] Rajakumar G, Thiruvengadam M, Mydhili G, Gomathi T, Chung IM. Green approach for synthesis of zinc oxide nanoparticles from Andrographis paniculata leaf extract and evaluation of their antioxidant, anti-diabetic, and anti-inflammatory activities. Bioprocess Biosyst Eng. 2018 Jan;41(1):21-30. https://doi.org/10.1007/s00449-017-1840-9

[10] Chandrasekaran S, Anbazhagan V, Anusuya S. Green route synthesis of ZnO nanoparticles using Senna auriculata aqueous flower extract as reducing agent and evaluation of its antimicrobial, antidiabetic and cytotoxic activity. Appl Biochem Biotechnol. 2023 Jun;195(6):3840-3854. https://doi.org/10.1007/s12010-022-03900-0

[11] V.C. Senthilkumar, N. Bhadusha, R. Uthrakumar, K, Kaviyarasu. Green synthesis of zine oxide nanoparticles dopped Leucas aspera leaf extract and its photocatalytic applications. Journal of Optoelectronic and Biomedical Materials 16(4): 189-197. https://doi.org/10.15251/JOBM.2024.164.189

[12] Tsegahun E, Aklilu M. Neem (Azadirachta indica) leaf extract mediated synthesis of zinc oxide nanoparticles (ZnO NPs) and their antibacterial activity. Discov Nano. 2025 Aug 22;20(1):145. https://doi.org/10.1186/s11671-025-04260-4

[13] Sarwar, K., Nazli, ZiH., Munir, H. *et al.* Biosynthesis of zinc oxide nanoparticles using *Moringa oleifera* leaf extract, probing antibacterial and antioxidant activities. *Sci Rep* **15**, 20413 (2025). https://doi.org/10.1038/s41598-025-08839-w

[14] M. Ramesh, M. Anbuvannan, G. Viruthagiri. Green synthesis of ZnO nanoparticles using Solanum nigrum leaf extract and their antibacterial activity, Spectrochimica Acta Part A: Molecular and Biomolecular Spectroscopy, Volume 136, Feb-2015, Pages 864-870, ISSN 1386-1425, https://doi.org/10.1016/j.saa.2014.09.105

[15] Gnanasekaran R., D. Yuvaraj, G. Koteswara Reddy, S. Naveen Shangar, V. Vijayakumar, J. Iyyappan. Zinc oxide nanoparticles from leaf extract of Eclipta prostrata: Biosynthesis and characterization towards potential agent against film forming bacteria in metal working fluids. Environmental Chemistry and Ecotoxicology, Volume 6,2024, Pages 206-215, ISSN 2590-1826. https://doi.org/10.1016/j.enceco.2024.06.001

[16] Sunil Christudas, TM Kulathivel, P Agastian. Phytochemical and antibacterial studies of leaves of Tridax procumbens L., Asian Pacific Journal of Tropical Biomedicine, Volume 2, Issue 1, Supplement, 2012, Pages S159-S161, ISSN 2221-1691, https://doi.org/10.1016/S2221-1691(12)60149-X

[17] Agrawal, S., Mohale, D., Talele, G.S., 2010. Pharmacological activities of Tridax procumbens (Asteraceae). Med. Plants - Int. J. Phytomed. Relat. Ind. https://doi.org/10.5958/ j.0975-4261.2.2.012

[18] Varsharani V. Ingole, Pravin C. Mhaske, Sushma R. Katade, Phytochemistry and pharmacological aspects of Tridax procumbens (L.): A systematic and comprehensive review, Phytomedicine Plus, Volume 2, Issue 1, 2022, 100199, ISSN 2667-0313, https://doi.org/10.1016/j.phyplu.2021.100199

[19] Singh, C.P., Mishra, P.K., Gupta, S.P., 2016. Design and formulation of Tridax procumbens based polyherbal cream for wound healing potential. Pharm. Lett. 8, 15–21. http://scholarsresearchlibrary.com/archive.html

[20] Verma, R.K., Gupta, M.M., 1988. Lipid constituents of Tridax procumbens. Phytochemistry 27 (2), 459–463. https://doi.org/10.1016/0031-9422(88)83120-0

[21] Beck, S., Mathison, H., Todorov, T., Calderon-Juarez, E.-A., Kopp, O.R., 2018. A review of medicinal uses and pharmacological activities of Tridax procumbens (L.). J. Plant Stud. 7. https://doi.org/10.5539/jps.v7n1p19

[22] Saxena, V.K., Albert, S., 2005. β-Sitosterol-3-O-β D-xylopyranoside from the flowers of Tridax procumbens Linn. J. Chem. Sci. 117, 263–266. https://doi.org/10.1007/ BF02709296

[23] Saraf, S., Pathak, A.K., Dixit, V.K., 1991. Hair growth-promoting activity of Tridax procumbens. Fitoterapia 62, 495–498.

[24] Sathya Bama, S., Jayasurya Kingsley, S., Sankaranarayanan, S., Bama, P., 2012. Antibacterial activity of different phytochemical extracts from the leaves of T. procumbens Linn.: identification and mode of action of the terpenoid compound as antibacterial. Int. J. Pharm. Pharm. Sci. 7, 1451–1460.

[25] Bray F, Ferlay J, Soerjomataram I, Siegel RL, Torre LA, Jemal A. Global cancer statistics 2018: GLOBOCAN estimates of incidence and mortality worldwide for 36 cancers in 185 countries. CA Cancer J Clin. 2018 Nov;68(6):394-424. https://doi.org/10.3322/caac.21609.

[26] Govindasamy Sharmila, Marimuthu Thirumarimurugan, Chandrasekaran Muthukumaran. Green synthesis of ZnO nanoparticles using Tecoma castanifolia leaf extract: Characterization and evaluation of its antioxidant, bactericidal and anticancer activities. Microchemical Journal, Volume 145, 2019, Pages 578-587, ISSN 0026-265X. https://doi.org/10.1016/j.microc.2018.11.022.

[27] Gupta A, Srivastava P, Bahadur L, Amalnerkar DP, Chauhan R (2015) Comparison of physical and electrochemical properties of ZnO prepared via different surfactant-assisted precipitation routes. Appl Nanosci 5:787–794 DOI: 10.1007/s13204-014-0379-1

[28] Bala, N.; Saha, S.; Chakraborty, M.; Maiti, M.; Das, S.; Basu, R.; Nandy, P. Green synthesis of zinc oxide nanoparticles using Hibiscus subdariffa leaf extract: Effect of temperature on synthesis, anti-bacterial activity and anti-diabetic activity. RSC Adv. 2015, 5, 4993–5003

[29] T.S. Anvekar, V.R. Chari, H. Kadam, Mat. Sci. Res. India. 14 (2017) 153–157. http://dx.doi.org/10.13005/msri/140211

[30] S. Talam, S.R. Karumuri, N. Gunnam, ISRN Nanotechnol. (2012)372505.

[31] R. Vijayalakshmi, V. Rajendran, Arch. Appl. Sci. Res. 4 (2012) 1183–1190 http://scholarsresearchlibrary.com/archive.html

[32] Rafael Álvarez-Chimal, Víctor Irahuen García-Pérez, Marco Antonio Álvarez-Pérez, Jesús Ángel Arenas-Alatorre, Green synthesis of ZnO nanoparticles using a Dysphania ambrosioides extract. Structural characterization and antibacterial properties, Materials Science and Engineering: Volume 118, 2021, 111540, ISSN 0928-4931, https://doi.org/10.1016/j.msec.2020.111540

[33] Khan, A.U., Malik, N., Singh, B. *et al.* Biosynthesis, and characterization of Zinc oxide nanoparticles (ZnONPs) obtained from the extract of waste of strawberry. *J.Umm Al-Qura Univ. Appll. Sci.* **9**, 268–275 (2023). https://doi.org/10.1007/s43994-023-00038-5

[34] Fakhari, S., Jamzad, M., & Kabiri Fard, H. (2019). Green synthesis of zinc oxide nanoparticles: a comparison. *Green Chemistry Letters and Reviews*, *12*(1), 19–24. https://doi.org/10.1080/17518253.2018.1547925

[35] Vinayagam, R., Pai, S., Murugesan, G. *et al.* Synthesis of photocatalytic zinc oxide nanoflowers using *Peltophorum pterocarpum* pod extract and their characterization. *Appl Nanosci* **13**, 847–857 (2023). https://doi.org/10.1007/s13204-021-01919-z

[36] Ubaithulla Baig A, Vadamalar R, Vinothini A, Fairose S, Gomathiyalini A, Jabena Begam N, Shaista Jabeen. Facile green synthesis of silver doped ZnO nanoparticles using Tridax Procumbens leaf extract and their evaluation of antibacterial activity. Journal of water and Environmental Nanotechnology. Volume-5 issue-4,2020,pages 307-320: https://doi.org/10.22090/jwent.2020.04.002

[37] Sirelkhatim, A. et al. Review on zinc oxide nanoparticles: Antibacterial activity and toxicity mechanism. Nano-Micro Lett. 7, 219–242. https://doi. org/ 10. 1007/ s40820- 015- 0040-x (2015)

[38] Soltanian, S. et al. Biosynthesis of zinc oxide nanoparticles using hertia intermedia and evaluation of its cytotoxic and antimicrobial activities. https://doi. org/10. 1007/ s12668- 020- 00816-z/ Publi shed

[39] Sirelkhatim A, Mahmud S, Seeni A, Kaus NHM, Ann LC, Bakhori SKM, Hasan H, Mohamad D. Review on Zinc Oxide Nanoparticles: Antibacterial Activity and Toxicity Mechanism. Nanomicro Lett. 2015;7(3):219-242. https://doi.org/10.1007/s40820-015-0040-x

[40] A. Saraste and K. Pulkki, Morphologic and biochemical hallmarks of apoptosis. Cardiovasc Res. 2000, 45 (3), 528-537. https://doi.org/10.1016/ s0008- 6363(99) 00384-3

[41] Wang C, Hu X, Gao Y, Ji Y. ZnO Nanoparticles Treatment Induces Apoptosis by Increasing Intracellular ROS Levels in LTEP-a-2 Cells. Biomed Res Int. 2015; 2015:423287. Epub 2015 Aug 3. PMID: 26339612; PMCID: PMC4538331 https://doi.org/10.1155/2015/423287